


See discussion, stats, and author profiles for this publication at: <https://www.researchgate.net/publication/390138794>


Thermospheric Response and Operational Impacts during the 2024 Gannon Geomagnetic Storm

Poster · November 2024
DOI: 10.1109/APS.2024.10944280

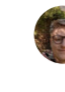
CITATIONS
0

7 authors, including:

 Charles Constant
University College London
11 PUBLICATIONS 3 CITATIONS
[SEE PROFILE](#)

 Sarthak Bhattacharjee
University College London
29 PUBLICATIONS 28 CITATIONS
[SEE PROFILE](#)

READS
136

 Indigo Brownfull
University College London
18 PUBLICATIONS 4 CITATIONS
[SEE PROFILE](#)

Thermospheric Response and Operational Impacts during the 2024 Gannon Geomagnetic Storm

Charles Constant, Indigo Brownhall, Laura Aguilar, Eliot Dable, Marek Ziebart, Anasuya Aruliah, Santosh Bhattarai
Space Geodesy and Navigation Laboratory & Atmospheric Physics Laboratory, University College London

Problem:

Approximately one-quarter of all Earth orbiting objects reside within the 100–800 km altitude band, where uncertainties in atmospheric density modelling present the dominant source of error in critical operational processes such as orbit prediction and collision risk assessment. These inaccuracies and their associated uncertainties are exacerbated during geomagnetic storms.

We aim to shed light on the nature of these errors by characterizing the impact of the Gannon storm in three operationally relevant questions:

1. How do physics-based and empirical thermospheric density models compare in terms of accuracy during storm periods?
2. How resilient are uncooperative tracking systems to the rapid changes in thermospheric density during storms?
3. What is the range of altitudes over which thermospheric variability significantly affects the orbital population, and how far beyond current assumptions does this extend?

Opportunity:

The Gannon storm is the first of its magnitude to unfold in such a densely populated orbital environment, making it crucial to characterize its operational impacts. As the orbital environment grows increasingly congested, future storms are likely to be even more impactful. The insights gained from this storm are of high relevance for improving preparedness and response to future events like this one.

In the absence of direct thermospheric measurements, this study integrates multiple independent, indirect sources of data to piece together a more informed understanding of storm-time dynamics. These include uncooperative satellite orbits, precise satellite orbits, and ground-based Fabry-Perot Interferometer measurements.

By quantifying the storm's impact through these methods, we aim to provide answers to our three key questions in a way that can directly inform satellite operators' decision-making processes.

Solar and Geomagnetic Drivers

The Gannon storm is the strongest geomagnetic storm in terms of Disturbance Storm Time (Dst) index after the 1989 and 2003 storms, with the Dst index peaking at -412 nT and remaining below -250 nT for over 23 hours. Following at least 6 Coronal Mass Ejections (CMEs), sudden storm commencement (SSC) occurred on 10 May 2024 at 16:45 UTC. Auroras were observed as far south as 23.2°N magnetic latitude. A strong interplanetary magnetic field (IMF) Bz component (with a maximum of -40 nT) and auroral electrojet (AE) index (peaking at 4000 nT) were indicative of a high geo-effectiveness of this event.

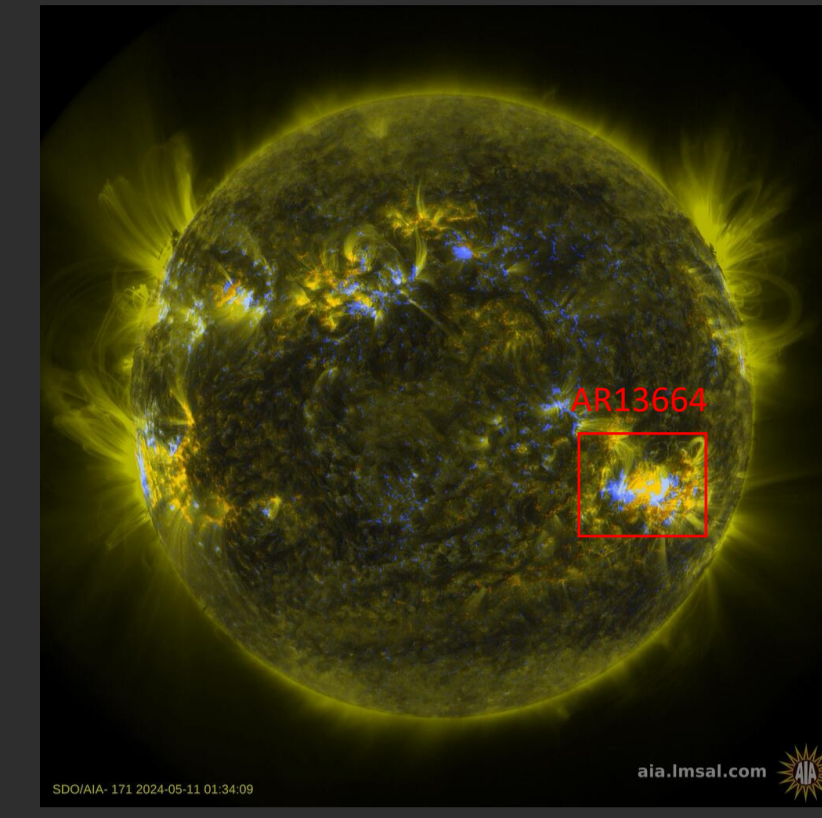


Figure 1. Coloured magnetogram of the Sun 14 minutes prior to the launch of the fastest (2015km/s) and most powerful flare (X5.9) from AR 13664 (NASA SDO Server)

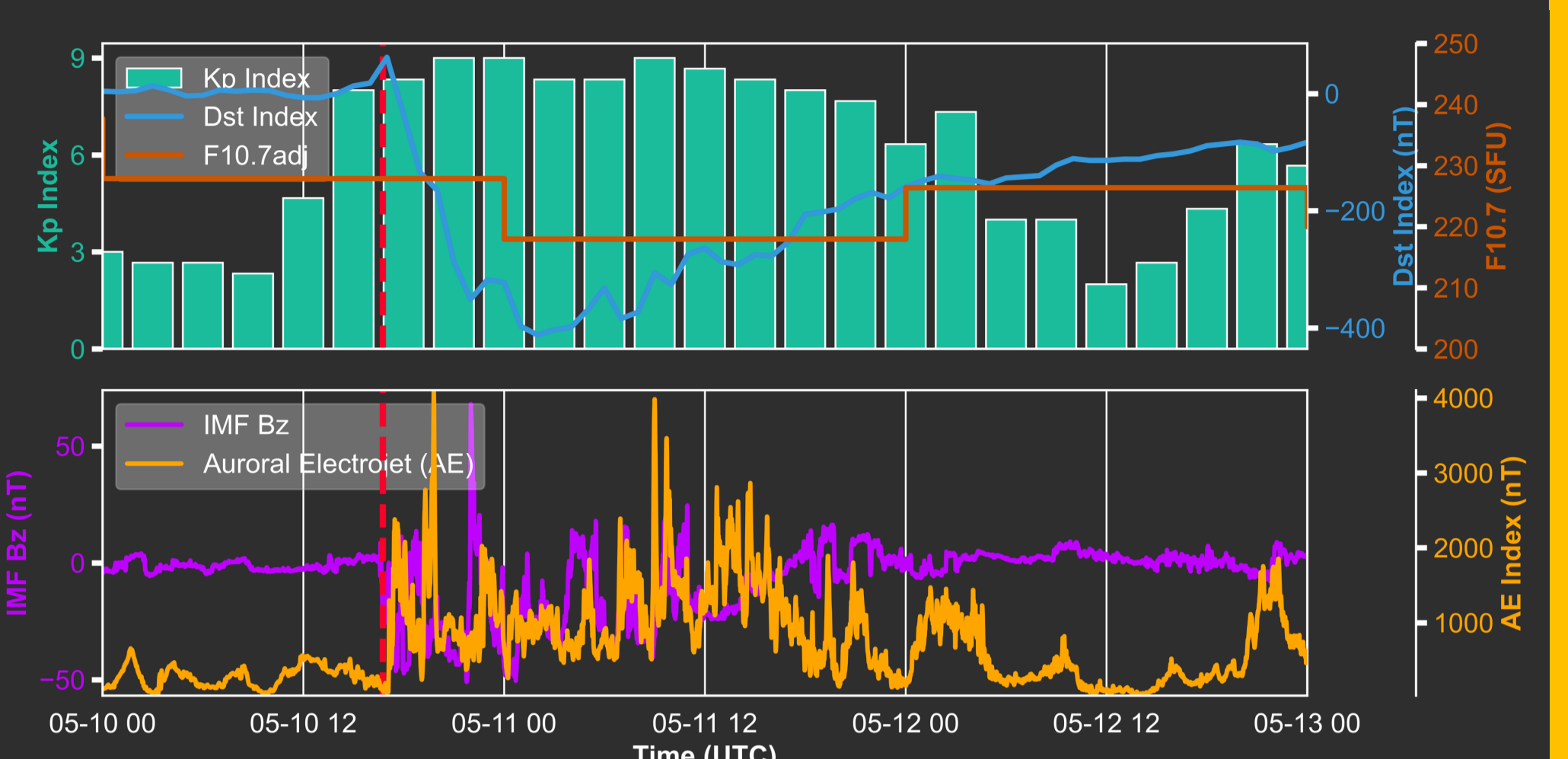


Figure 2. Key space weather indices between the 10th and 13th of May 2024

In-Orbit Density Observations

Method: Reference densities were retrieved from a POD-accelerometry process using near-real time orbits from the Potsdam FTP server (GRACE-FO + TerraSAR) and the Copernicus Data Space Environment (Sentinel-1A/2A)

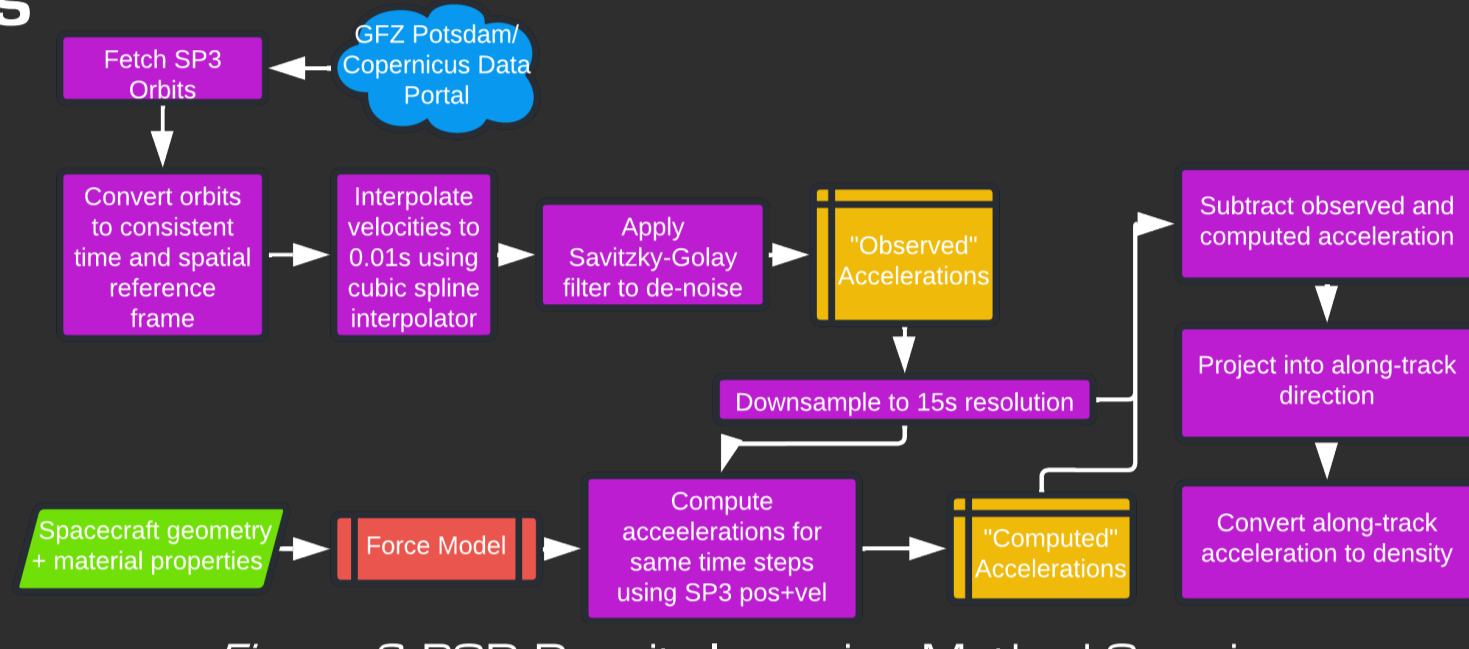


Figure 3. POD Density Inversion Method Overview

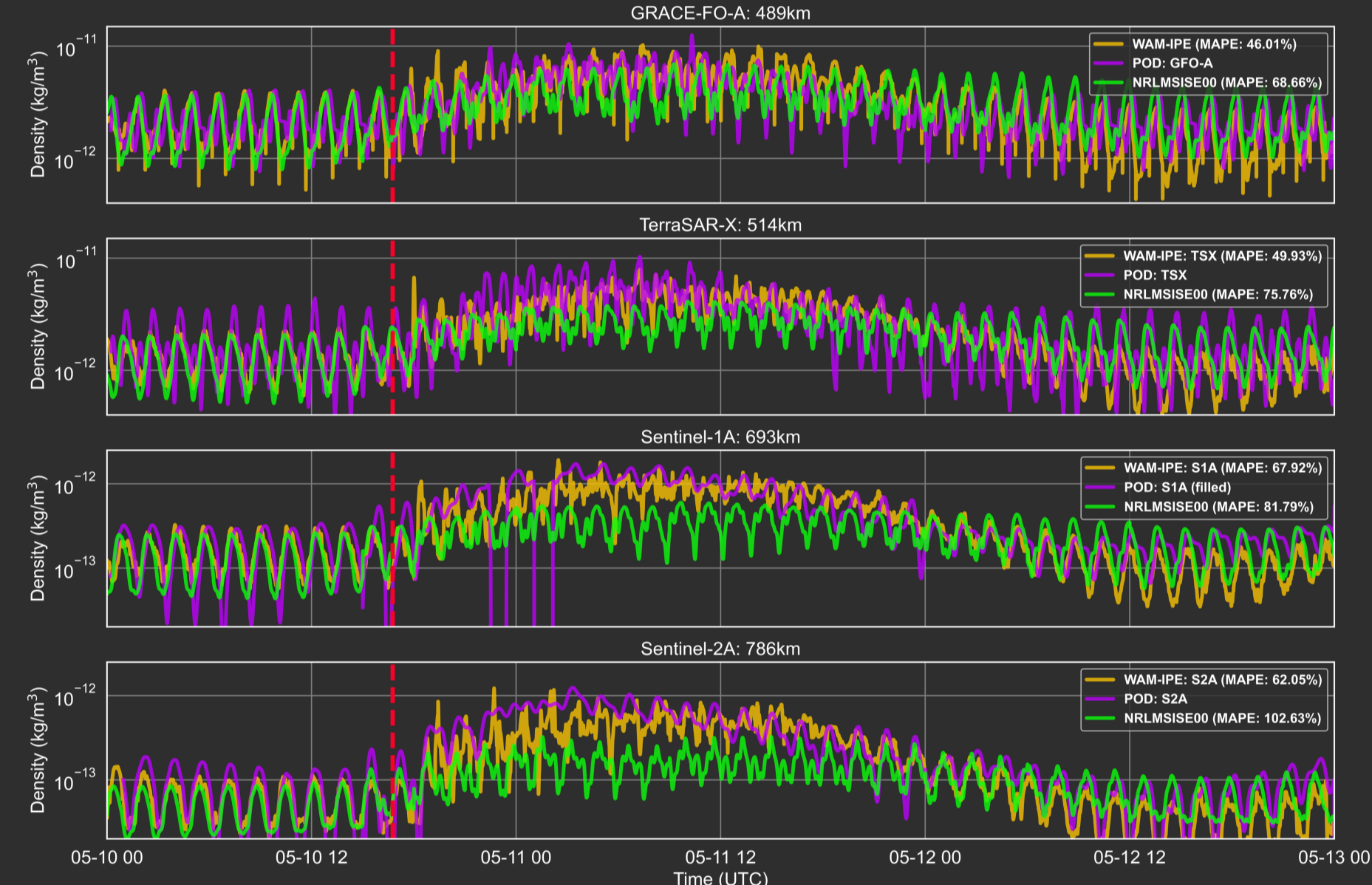


Figure 4. Time series of densities retrieved using POD, WAM-IPE and MSISE-00 for GRACE-FO-A, TerraSAR-X, Sentinel-1A, and Sentinel-2A over the course of the storm

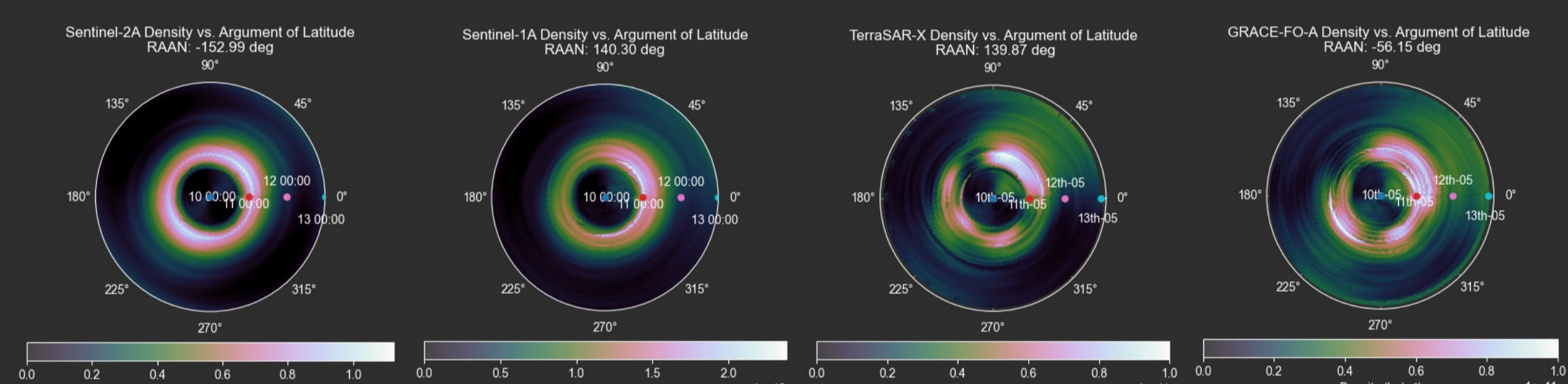


Figure 5. Circular plots of the density as a function of the argument of latitude for the four satellites studied. Time spirals outwards with each colored dot representing a new day between the 10th and 13th of May.

Physics vs Empirical Model Performance:

- WAM-IPE captures the duration and intensity, and resolution of the storm features better at all altitudes.
- MSISE-00 performs worse in capturing the intensity of the density increase at higher altitudes and the post-storm cooling at lower altitudes.
- At lower altitude, all models perform worse in Mean Absolute Percentage Error terms.

Ground-Based Density, Temperature and Wind Observations

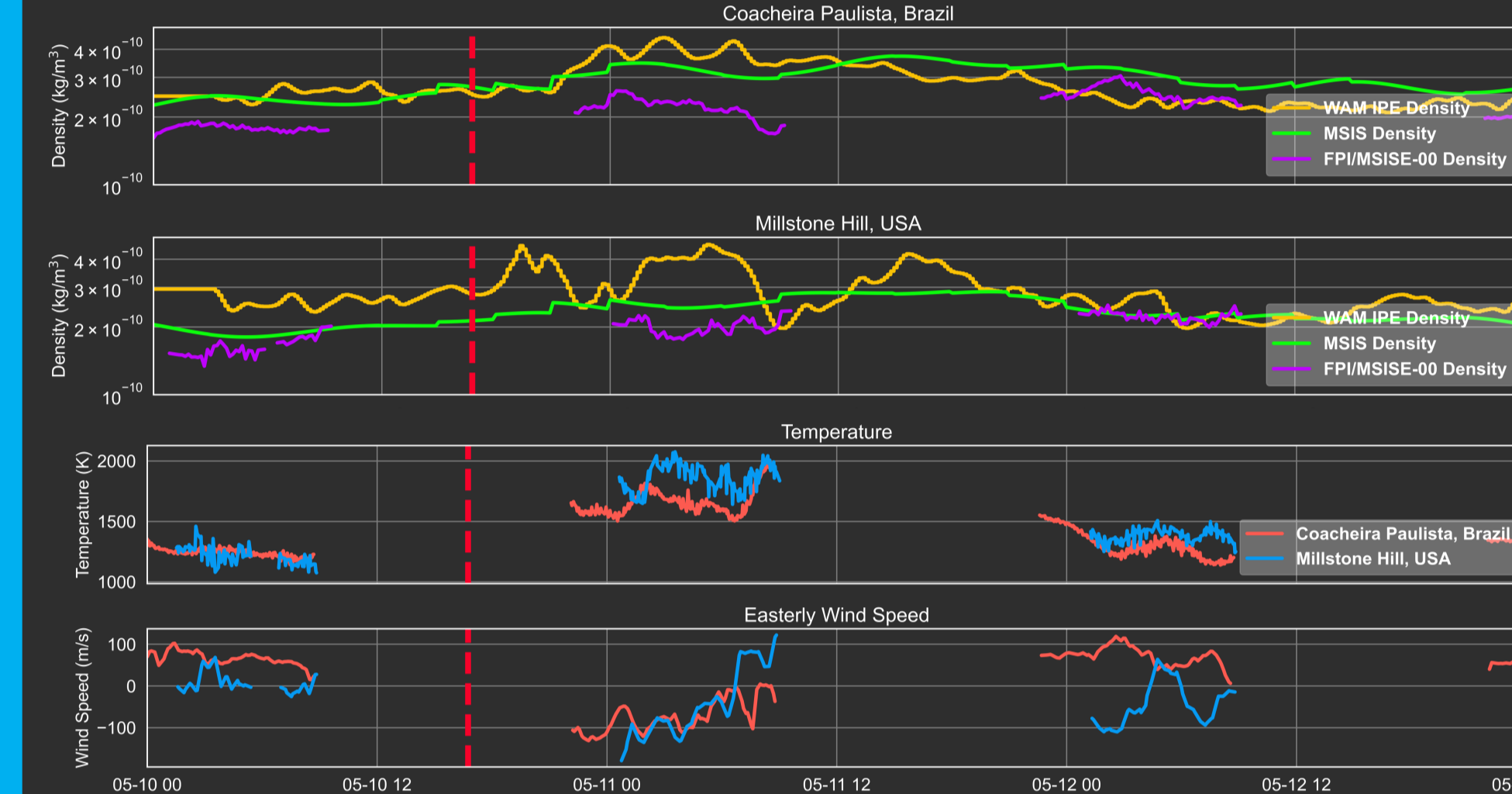


Figure 6. FPI Derived densities, temperatures and winds at the Millstone Hill and Coacheira Paulista sites

FPI-derived densities, were generated using the measured FPI temperature T_{FPI} , as well as the temperature from a model T_{model} , in this instance NRLMSIS-00 was selected. In addition, the number density N_i , and molar masses M_i , of each of the different species were used to generate density ρ_{FPI} . The equation is shown below:

$$\rho_{FPI} = \frac{k_b T_{model}}{RT_{FPI}} \sum_i N_i M_i$$

Where k_b is the Boltzmann constant and the ideal gas constant is R. This method provides an FPI-derived density that adjusts the model density by accounting for temperature variations measured by the FPI.

- We see a 6x increase in wind speed in North-East USA, for South Brazil the increase was minimal.
- There was a 40% increase in temperature after the onset of the storm in Brazil, and a roughly 60% increase in the North-East USA.
- In both the USA and Brazil, we see the large increase in temperature and density occur simultaneously. FPI calculated density takes longer to reach the peak than both the WAM-IPE and MSIS models. Temperatures fell back to baseline within a day for the Brazil site but took 2 days for the US site. Easterly wind speeds took a day to recover to baseline for both sites.

Storm impacts on the thermosphere

- For both FPIs, in Brazil and the USA, the FPI density is lower than the model densities, sometimes as much as 2 times lower at 210km altitude.
- The storm had an impact on the temperature easterly wind speeds in the lower thermosphere – seen more strongly at lower latitudes.
- During the latter part of the main phase of the storm, a noticeable reduction in orbit derived neutral density occurred, likely due to NO cooling. This was visible as the storm lasted long enough for NO cooling effects to become evident while the main phase was still ongoing.
- Storm onset seems more sudden and stronger (in relative terms) at higher altitudes
- Relative increase in once-per rev density is up to an order of magnitude for Sentinel-2A, which is explained by the fact that it was orbiting with its day side at local solar noon.

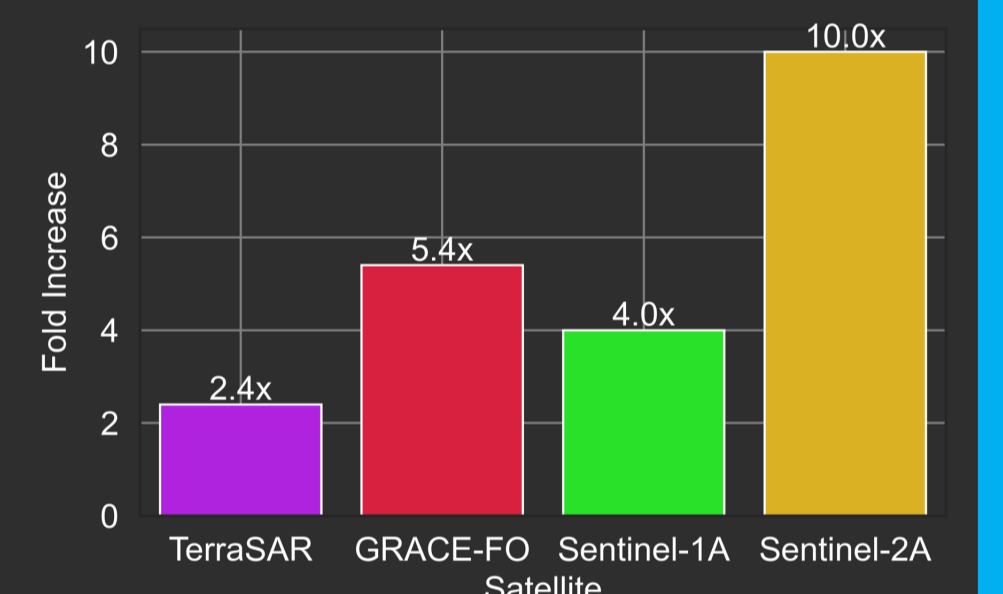


Figure 7. Peak increase in once-per-rev POD-derived density relative to pre-storm densities.

Observed Altitude Decay in Resident Space Objects

Method:

- We analysed the entire space-track.org Two Line Element (TLE) orbital catalogue, comprising 26,169 objects, restricting altitude data to ≤ 1000 km and excluding manoeuvring objects—defined as those whose mean orbital altitude increases by >100 m within a 3-hour window, thereby omitting 9,821 objects.
- Post-storm, numerous satellites exhibited altitude decay in response to the increased atmospheric density. We sampled satellites in Low Earth Orbit (LEO) with altitudes between 480 km and 870 km to model their immediate and prolonged decay in Semi-Major Axis values.
- Furthermore, we calculate the daily altitude change (km/day) for all objects to quantitatively ascertain the altitude at which atmospheric drag most significantly affects LEO trajectories.

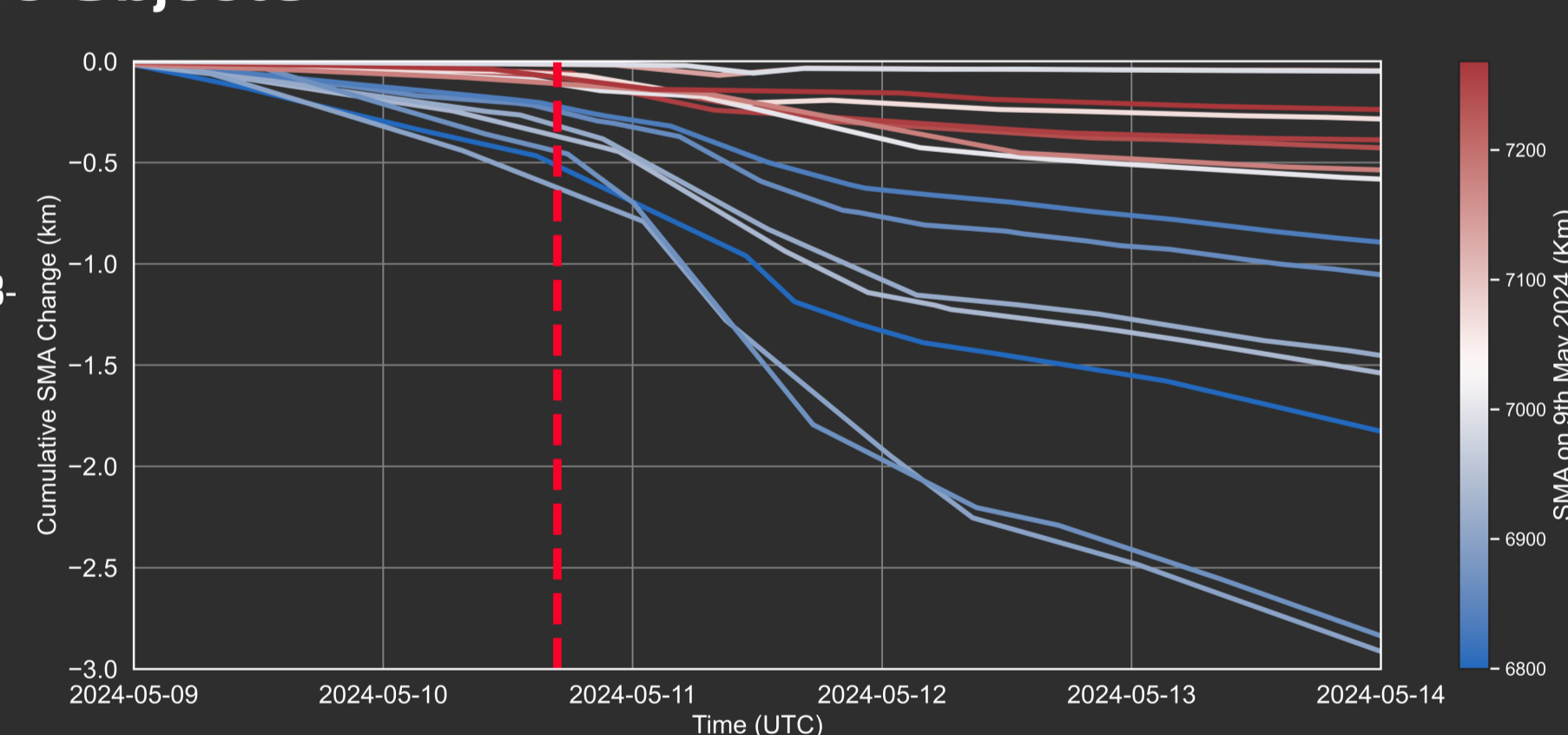


Figure 8. Cumulative decay in semi major axis for select NORAD IDs around the period of the storm

Result:

- Beyond a long-term increase in the rate of altitude decay after the storm, the selected LEO satellites also experienced sudden altitude drops during the storm. The daily change in SMA for these satellites shows a sudden altitude drop spanning between 100m to 1.4km during the storm.
- Although most objects seem to have SMA rate of change values clustered around 0km/day, their decay most commonly lies between 0-0.5km, where a significant number of data show shrinking orbits for most LEO objects of the catalogue.
- Some indicate more rapid orbital decay and aggressive manoeuvres. Showcasing orbital stability variations depending on the object under consideration.

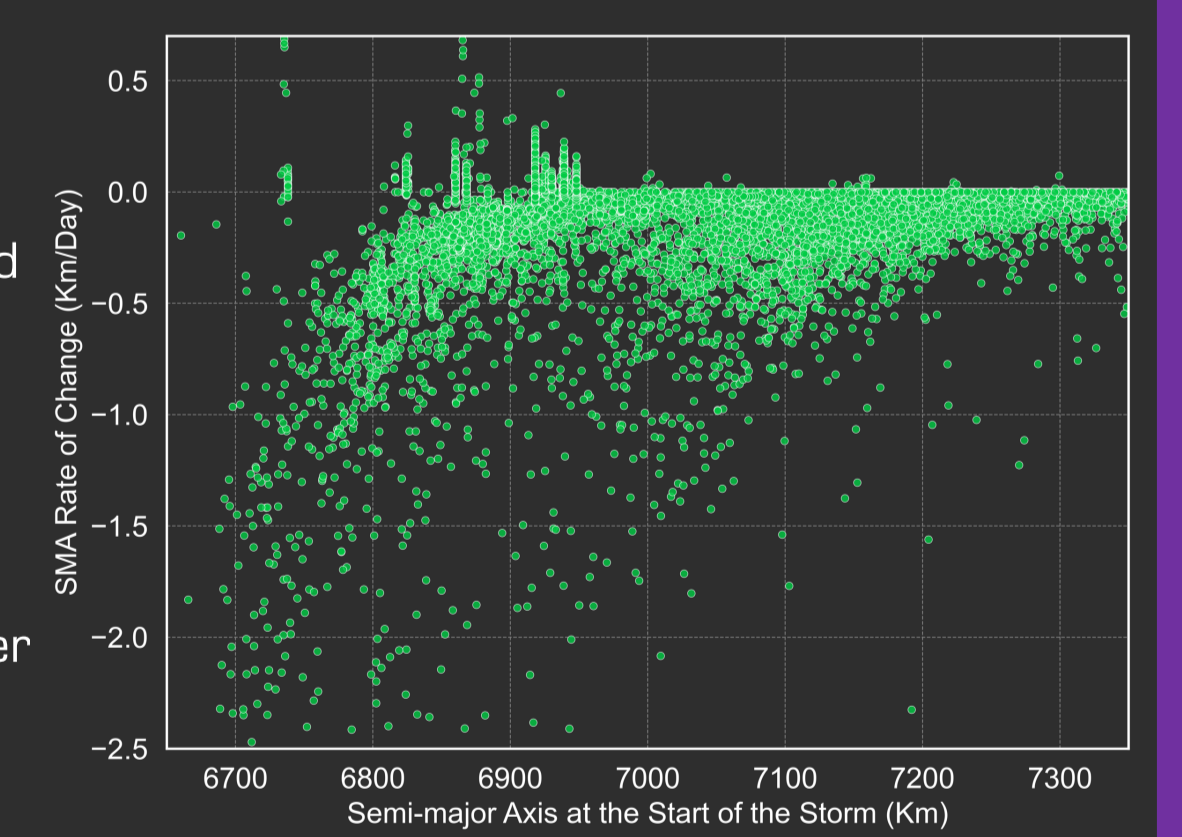


Figure 9. Rate of change in SMA over the period of the storm for all objects in the space-track catalog between 300-1000km altitude.

Degradation in Uncooperative Tracking Accuracy

Method: To measure tracking accuracy degradation, we compared TLE-based orbits with precise orbit data during the storm. TLEs were propagated with SGP4 to simulate the tracking fidelity of TLE-based, uncooperative systems. For the same period, Rapid Science Orbits are pulled from the GFZ Potsdam FTP server and stitched together to form a continuous reference ephemeris. Given this data is accurate on the level of a few centimetres, we use the relative difference between the two sets of orbits as a measure of accuracy.

Result: Much of the recorded error appears in the orbit along-track direction ($>80\%$). For the 48 hours following SSC, we notice a marked degradation in the uncooperative orbits of all the satellites. While the error drops down when new TLEs are made available it quickly degrades again. While the along-track error shows a negative trend (over-prediction of drag) for GRACE-FO-A and Sentinel-2A, TerraSAR-X and Sentinel-1A display a positive trend instead. Overall, we see a 2-4-fold increase in the tracking error between the pre-storm and storm phases. This is roughly commensurate with the recorded increases in POD-derived density. All satellites are in error by multiple kilometres at some stage. This is 1-2 orders of magnitude beyond the sought level of tracking accuracy by current SSA/STM systems (± 100 s meters).

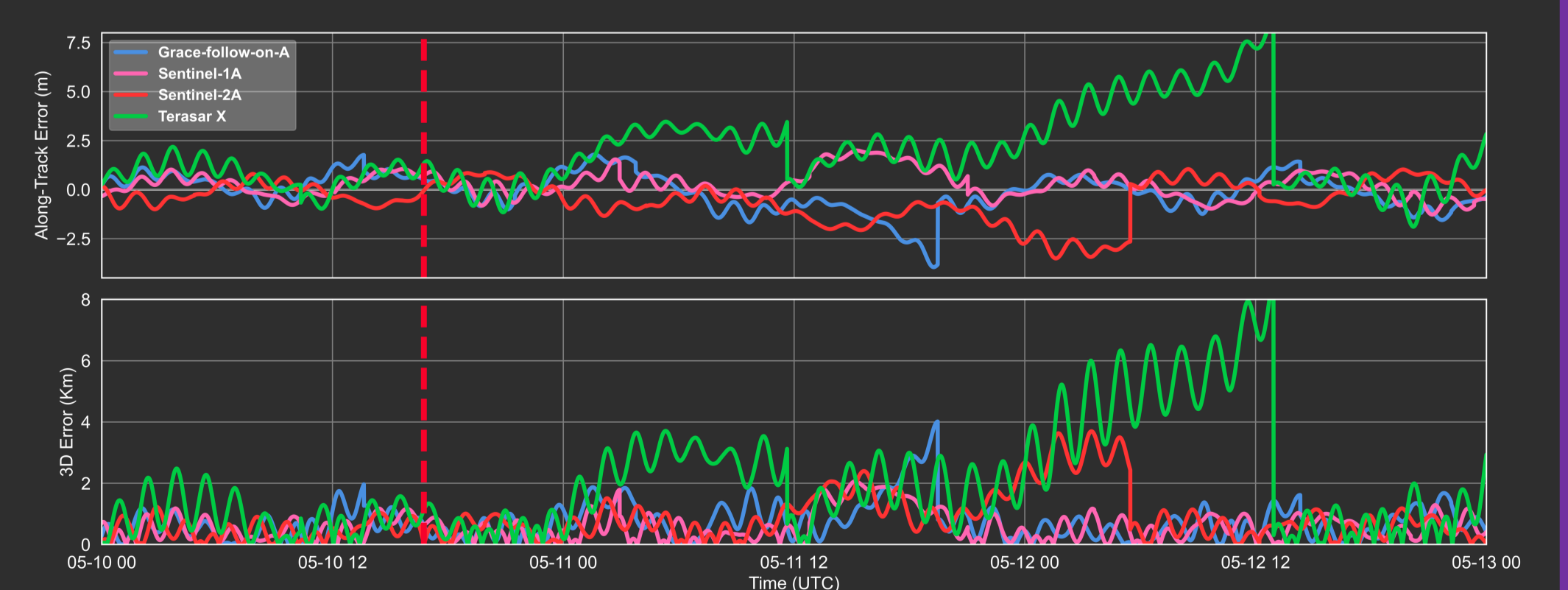


Figure 10. 3D absolute difference (top) and along-track component of difference (bottom) between TLE-derived and SP3 ephemerides

Operational impacts of the storm

- Physics-based density models emerge as a promising operational tool for density modelling. They capture the behaviour of the storm with high-accuracy.
- Ground-based observations of the temperature and winds illustrate the intensity of the storm and show some disagreement with empirical model temperatures
- Tracking quality suffered a relative 2-4x degradation in positional accuracy compared to pre-storm levels.
- Drag effects were observed up to 1000km altitude using uncooperative tracking data. It is likely atmospheric drag effects were significant beyond this altitude.
- Whilst the orbital environment is highly crowded, no major incidents were linked to this event.

